ISSN: 2753-7919
British Journal of Healthcare and Medical Research; Vol. 13 No. 05 (2026) (293-300)
https://doi.org/10.14738/bjhr.1305.12225

# The Kinetics of Deprivation: Unifying Early Life with the Gompertz-Makeham Law of Mortality

Bernard Silke

Department of Internal Medicine, St James's Hospital & Department of Therapeutics, Trinity Centre, Dublin 8, Ireland

**Abstract**: Background: Socio-economic deprivation is associated with higher mortality. In a previous adult life-table analysis, deprivation-related loss of life years was represented by an approximately fixed horizontal age shift in mortality risk: 12 years in males and 9 years in females across ages 40–85. Within the Gompertz component, this was associated with approximately constant standardised mortality ratios. Childhood studies have reported associations between social adversity and early-life biological differences, including altered leukocyte telomere dynamics. The relation between these early-life observations and the approximately fixed adult mortality shift is uncertain. Aim: To develop an illustrative life-course model showing how an age shift emerging in early life could travel from zero at birth to the approximately fixed adult displacement used in the mortality analysis, and to examine the resulting rate and acceleration profile. Methods: A continuous sigmoidal function was used to represent accumulation of the modelled age shift, $\Delta(t)$, from zero at birth towards the sex-specific adult shifts. The trajectory was specified to increase gradually in early life, more rapidly through childhood and adolescence, and then decelerate as it approached the adult level. The adult shifts were 12 years in males and 9 years in females. Rates of change and acceleration were examined as properties of the illustrative function. Results: A linear transition from childhood to the adult age shift produced an abrupt change in slope. In contrast, the sigmoidal function generated a smooth trajectory, with a low initial rate of accumulation, more rapid change through later childhood and adolescence, and progressive deceleration thereafter. The modelled trajectory was close to its adult level by the mid-thirties. In the adult life-table analysis, the resulting fixed shifts produced absolute annual mortality-risk differences that increased with age, despite the approximately constant relative mortality effect within the Gompertz component. Conclusion: A simple continuous function can provide a mathematical illustration of how early-life divergence could approach the approximately fixed age shift observed in mature adult mortality. $\Delta(0) = 0$ at birth is used as a mathematical starting condition consistent with the adult boundary, not as a claim that biological divergence begins at birth, and the modelled timings depend on the calibration anchors chosen. The model does not identify an underlying biological mechanism or estimate the timing of real-world biological change. It provides a conceptual framework for considering how disadvantage across the life course may be related to later mortality inequalities.

**Keywords:** Deprivation, Gompertz-Makeham, life years lost (LYL)

## INTRODUCTION

Deprivation was defined by Townsend as a state of observable and demonstrable disadvantage relative to the local community to which an individual belongs (1) and is associated with increased population mortality (2, 3). In deprived populations, life expectancy has improved only modestly over time - by 4.0 years in males and 2.6 years in

females between 1970 and 2010 in one linked-data analysis. However, substantial socioeconomic disparities have persisted (4, 5). Reported deprivation-associated mortality ratios have ranged from approximately 1.2 to 3.6, depending on age, cause of death, and the definition and severity of deprivation (1, 6).

In a previous modelling analysis, deprivation-related LYL in mature adult life was consistent with earlier horizontal entry onto the mortality trajectory rather than with a progressively accelerating rate of ageing (7). This was represented as a biological-age advance Δ of 12 years in males and 9 years in females across ages 40–85. Within the pure Gompertz component, the corresponding SMR was approximately constant across this age range: 2.21 in males and 1.81 in females. However, this empirical constancy introduces an apparent life-course paradox. Recent longitudinal childhood studies suggest that social adversity may be associated with early-life biological differences, including altered leukocyte telomere dynamics (8). If deprivation-related mortality risk is already fixed by age 40, as suggested by the approximately constant adult SMR in our previous analysis (7), a simple question follows: when, and by what trajectory, did that shift accumulate? By construction, the divergence must be zero at birth and reach the adult value (12 years in males, 9 years in females) before age 40. The intervening course is not observed and cannot be inferred from an adult life table alone.

The present paper addresses this question through hypothetical model-fitting rather than empirical validation. We use the post-40 age shift as a fixed adult boundary condition and set Δ(0) = 0 at birth as a mathematical starting condition, not as a claim that biological divergence begins at birth. The intervening course is represented by a continuous saturating function; a linear transition is not used, as it would produce a discontinuity in the rate of change at the adult boundary. Once shape parameters are chosen to satisfy two illustrative calibration anchors in the second and third decades, the function necessarily implies a particular trajectory - with low accumulation in early childhood, faster change through later childhood and adolescence, and deceleration through the twenties. This implied timing is a consequence of the selected parameters, not an independent estimate of when biological change actually occurs. Available evidence, including reports of altered leukocyte telomere dynamics in disadvantaged children (8), is compatible with an earlier onset, but the true starting age is not known and cannot be recovered from an adult life table.

## METHODS

### Model Framework and Boundary Conditions

This was a conceptual model providing a continuous representation of how the modelled age shift might accumulate before mature adult life. The selected function and parameter values were illustrative rather than fitted to individual-level longitudinal data.

The function $\Delta(t)$ represents the cumulative horizontal age shift at chronological age $t$. It was specified with Δ(0) = 0 as a mathematical boundary condition — not as an assertion that biological divergence begins at birth - and to approach the sex-specific adult shifts identified in the previous life-table analysis (7).

The functional form was chosen so that the trajectory could increase gradually in early life, more rapidly through childhood and adolescence, and decelerate as it approached

the approximately stable adult displacement represented in the post-40 mortality analysis; the specific rate and acceleration profile arising from this form is presented in the Results.

$$\Delta(t) = \begin{cases} f(t), & 0 \le t < 40 \\ 12.0 \text{ years (Males)}, & 40 \le t \le 85 \\ 9.0 \text{ years (Females)}, & 40 \le t \le 85 \end{cases}$$

The two matching conditions imposed at the adult boundary were:

$$\lim_{t \to 40} \Delta(t) = \Delta_{max} \text{ and } \lim_{t \to 40} \frac{d\Delta}{dt} = 0$$

These were used as approximate matching conditions to avoid a discontinuity in slope at the adult boundary; for a Hill-type saturating function they are approached rather than exactly attained at t = 40.

**Illustrative Saturating Function**

A non-linear saturating function was used to represent gradual accumulation of the modelled age shift during early life. This allowed the trajectory to begin close to zero at birth, increase more rapidly during childhood and adolescence, and then approach the adult level without the abrupt change in slope produced by a linear transition.

$$\Delta(t) = \Delta_{max} \frac{t^p}{h^p + t^p}$$

The function included three parameters:

- $\Delta_{max}$, the sex-specific adult age shift: 12 years in males and 9 years in females.
- $h$, the half-saturation parameter, representing the age at which the function reaches one half of its eventual value.
- $p$, the shape parameter, which controls how quickly the modelled shift rises and how sharply its rate of increase subsequently declines.

The difference between the male and female ceilings reflects the sex-specific adult shifts used in the preceding life-table analysis. It is a feature of the model specification, rather than an estimate of an underlying biological mechanism.

**Rate of Change and Acceleration**

The first and second derivatives of $\Delta(t)$ were calculated analytically to describe the rate of change and acceleration of the illustrative trajectory across childhood and early adult life: $\frac{\mathrm{d}\Delta(\mathrm{t})}{\mathrm{dt}}$ and $\frac{\mathrm{d}^2\Delta(\mathrm{t})}{\mathrm{dt}^2}$. These derivatives were used to generate Figure 3. They describe mathematical properties of the selected function and illustrate how the rate of accumulation changes over time; they are not empirical estimates of biological rates.

**Parameter Selection and Illustrative Milestones**

The parameters $\boldsymbol{h}$ and $\mathbf{p}$ were selected to produce an illustrative trajectory consistent with the proposed life-course pattern. The calibration anchors were chosen to approximate two-

thirds of the eventual shift by age 20 and about 90% by age 28. These corresponded to an age shift of about 8 years in males and 6 years in females at age 20, and about 11 years in males and 8 years in females at age 28.

Solving for these calibration points gave $p \approx 4.2$ and $h \approx 17.1$ years. Under this parameterisation, the modelled trajectory increases gradually in early life, more rapidly through childhood and adolescence, and then decelerates during the third decade as it approaches the adult displacement used in the post-40 mortality analysis. The calibration points were selected to illustrate this proposed trajectory. The specific timing of the modelled acceleration and peak velocity therefore depends on the choice of these two anchors; alternative anchor ages consistent with the same adult boundary condition would produce different implied trajectories.

## RESULTS

### Post-40 Absolute Mortality-Risk Differences

Figure 1 shows the absolute annual mortality-risk difference $(\Delta q_{x,s})$ generated by the fixed adult age shift. Discrete markers show the calculated sex-specific life-table coordinates obtained by applying a 12-year shift in males and a 9-year shift in females to Irish Life Table 17 baseline mortality. Although the pure Gompertz SMR was modelled as approximately constant after age 40, the absolute mortality-risk difference increased non-linearly as background mortality rose with age. Between ages 40 and 55, the difference remained below one percentage point in both sexes. Thereafter, it increased rapidly, reaching 20.5 percentage points in males and 7.8 percentage points in females at age 85. The separation between the curves reflects the smaller modelled age shift in females.

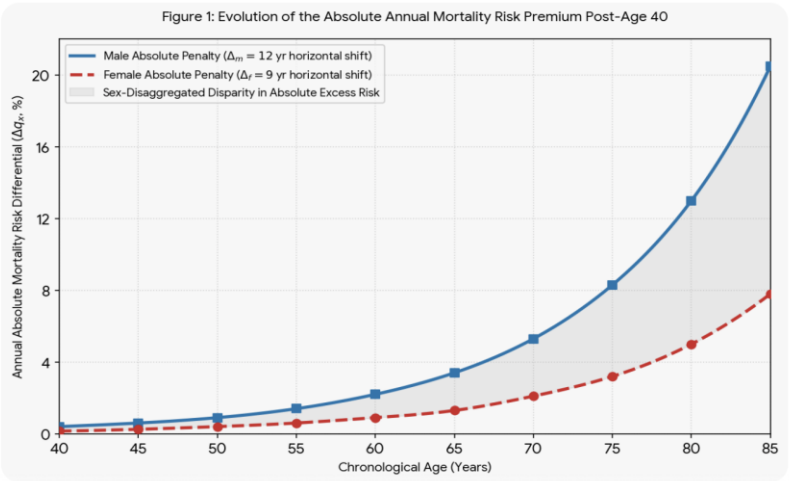



**Figure 1: Sex-specific absolute annual mortality-risk differences across adult life (ages 40-85), expressed as percentage points. Lines show the modelled trajectories; markers show calculated life-table coordinates.**

### Early-Life Accumulation of the Modelled Age Shift

Figure 2 illustrates the continuous accumulation of the modelled age shift, $\Delta(t)$, from birth towards the adult level used in the mortality analysis. A sigmoidal rather than linear

trajectory allows divergence to emerge gradually in early life, increase more rapidly through adolescence, and approach the approximately fixed age shift applied in the post-40 model. During the third decade, the rate of accumulation declines. By age 35, $\Delta(t)$ is close to its adult level while $d\Delta/dt$ has become relatively small, allowing the trajectory to converge on the approximately parallel adult Gompertz–Makeham pattern.

After childhood, the modelled shift increases more rapidly through adolescence. By age 20, the accumulated age shift is approximately 8 years in males and 6 years in females; by age 28, it is approximately 11 years in males and 8.25 years in females. The female trajectory follows the same relative temporal pattern, scaled to the lower female adult shift of 9 rather than 12 years.

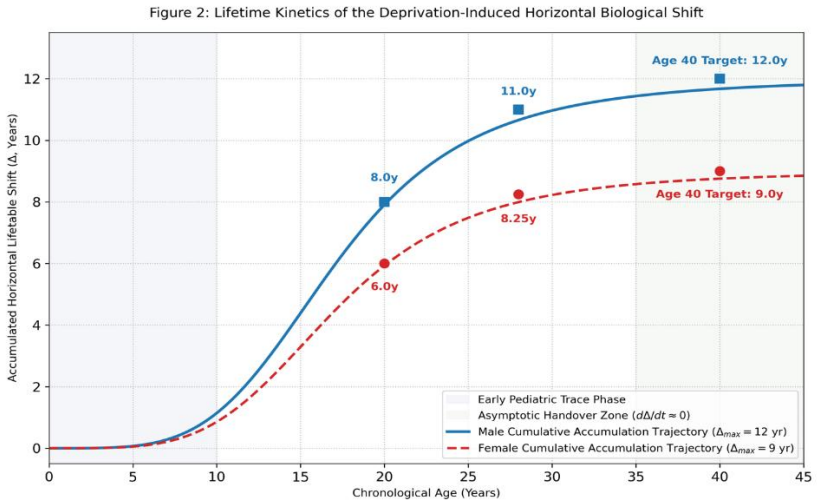



**Figure 2: Illustrative accumulation of the modelled age shift, $\Delta(t)$, from birth towards the adult level used in the mortality analysis. Lines show the illustrative sigmoidal trajectories. Square and circular markers indicate the approximate male and female values at ages 20 and 28. The shaded region indicates the later transition period, during which the rate of accumulation $d\Delta/dt$, declines as the trajectories approach their adult levels.**

### Rate of Change in the Illustrative Early-life Model

Figure 3 shows the rate of change and acceleration of the illustrative early-life accumulation function. In Panel A, the rate of change is low in early childhood, increases through later childhood, and reaches a maximum in adolescence. At this point, the modelled rate is approximately 0.75 years of age shift per chronological year in males and 0.56 years in females. Panel B shows the corresponding acceleration profile, which reaches an early maximum during childhood, crosses zero near the point of maximum rate of change, and is negative thereafter as the trajectory approaches its adult level. By approximately age 30, acceleration has declined substantially, indicating that the modelled rate of accumulation is slowing as it approaches the adult mortality pattern. These features are mathematical consequences of the selected function under the stated boundary conditions and are not empirical estimates of biological events.

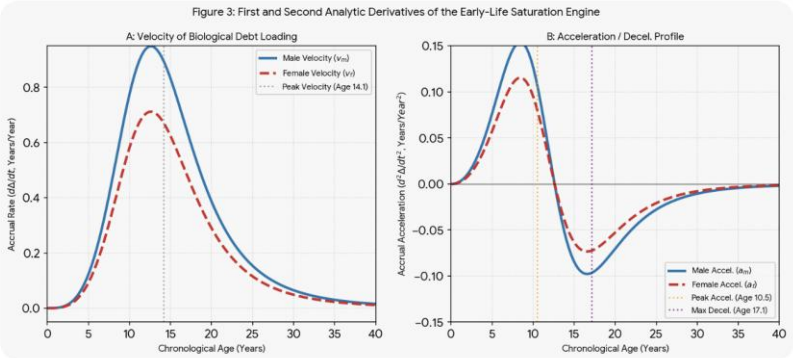



**Figure 3: Rate of change and acceleration of the illustrative early-life age-shift function. Panel A shows the age-specific rate of accumulation $d\Delta(t)/dt$, with the modelled rate reaching its maximum during adolescence. Panel B shows the corresponding acceleration profile $a(t) = td^2\Delta/dt^2$, illustrating the shift from increasing to decreasing accumulation rates as the trajectory approaches its adult level.**

## DISCUSSION

In our earlier life-table analysis, the deprivation-related SMR was approximately constant across ages 40–85, at about 2.2 in males and 1.8 in females (7). This adult mortality penalty is broadly consistent with the wider literature, which reports an approximately two-fold excess in all-cause mortality and higher excess risks for premature mortality (<65 years), cardiovascular disease, and avoidable deaths (9, 10), commonly attributed to ongoing adverse exposures, occupational stressors, and resource constraints operating across the adult lifespan (11). Social disadvantage is conceptually distinct from absolute material poverty (12), and the relative contributions of community-level circumstance and individual-level susceptibility remain unresolved (13). The relative stability of the adult SMR is not readily reconciled (7) with an ongoing accelerating process; if the relative mortality effect is already fixed by age 40, then exposures triggering such an effect must have occurred at an earlier life stage.

A central point of the present framework is that the adult mortality penalty is best interpreted as the settled outcome of a process that has largely completed by early adulthood, rather than as an endpoint that continues to accumulate through mid- and late life. Because the adult SMR is approximately fixed by age 40 (7), the substantive question shifts from a general enquiry into "socioeconomic determinants of mortality" to a more specific one: what trajectory during the first four decades of life is consistent with the adult boundary condition observed after age 40?

On this interpretation, the adult mortality penalty is best read as the settled outcome of an earlier accumulation process rather than as an active exposure operating in late life. The first and second derivatives of Δ(t) provide a way of describing how quickly the modelled shift accumulates and how that rate of accumulation changes with age. A linear accumulation would require a discontinuity at the adult boundary near age 40, since Δ(t) must transition from an increasing childhood trajectory to an approximately fixed adult value; a sigmoidal form allows this transition to occur smoothly. Reports of altered leukocyte telomere dynamics and other early biological differences in disadvantaged children (8) are consistent with an early onset of divergence, although the modelled

trajectory is illustrative and the true starting age cannot be recovered from an adult life table.

The illustrative parameterisation is conceptual and awaits empirical calibration. Within this parameterisation, the modelled process is initiated in childhood, with subsequent acceleration to a peak rate of accumulation in adolescence; these features are properties of the selected function under the stated boundary conditions and are not empirical estimates of biological events. Adolescence is nonetheless a plausible period of interest, given the biological and social transitions of that stage and the potential for exposures and structural disadvantage to interact with developing physiological systems. In the male trajectory, the accumulated shift reaches approximately 8 years by age 20 and about 11 years by age 28; the female trajectory follows the same relative temporal pattern, scaled to the lower adult female shift (approximately 6 years at age 20 and 8.25 years at age 28). This proportional scaling reflects the smaller adult age shift used for females (9 years, versus 12 years in males) and is consistent with the sex difference identified in our earlier analysis (7). Under this parameterisation, the greater part of the modelled adult age shift has accumulated by age 20, so most of the associated life-years lost is attributable to the pre-adult phase of the trajectory rather than to further accumulation in later life.

A further feature of the illustrative trajectory is that the rate of accumulation declines during the third decade of life, so that by age 35, $\Delta(t)$ is close to its adult level and $d\Delta/dt$ has become small. In mathematical terms this is what allows the model to reproduce an approximately fixed adult age shift ($\Delta_m = 12$ years, $\Delta_f = 9$ years) and an approximately constant adult SMR from age 40 onwards, without requiring any further contribution from adult exposures. Our earlier analysis indicated that most of the deprivation life-years lost accumulate before the end of the third decade, with approximately 11 years in males and 8 years in females already realised by around age 28 (7). Any candidate trajectory must therefore travel from $\Delta(0) = 0$ to close to the adult level over roughly the first three decades of life; among the small number of functional forms compatible with this constraint, a saturating accumulation of the type used here is more consistent with these constraints than either a linear or an exponential form, which would require a discontinuity at the adult boundary. Whether an analogous trajectory operates biologically, and whether it might in principle be modifiable, cannot be resolved from an adult life table and is outside the scope of the present analysis. The determinants that produce differences of this magnitude are deeply embedded in the social and family circumstances of early life, and their interpretation and any policy response lie beyond the reach of a mortality-modelling exercise.

**Limitations:** Several limitations should be noted. First, the analysis is based on a single national life table and a stylised deprivation model implemented as a fixed age shift; although this provides structural clarity, it does not capture heterogeneity in deprivation intensity, cohort effects, or cause-specific mortality. Second, the early-life trajectory is illustrative rather than empirically fitted: $\Delta(0) = 0$ is a mathematical starting condition consistent with the adult boundary rather than a claim about the biological age of onset, and the specific timing of the modelled acceleration depends on the calibration anchors chosen at ages 20 and 28 — alternative anchors consistent with the same adult boundary would produce different implied trajectories. Third, the analysis used relative life-years lost and their derivatives at five-year intervals without individual-level data on multimorbidity, behaviours, or biomarkers, so the model cannot distinguish between biological ageing

processes and selective survival as drivers of the observed trajectories. Finally, the sex-specific patterns described here arise from the geometry of the baseline Gompertz–Makeham schedules and the chosen age-shift parameters; their generalisability remains a hypothesis, requiring validation in other populations using empirical life tables and, ideally, longitudinal data linking deprivation exposure to individual survival paths.

## REFERENCES


1. Townsend P. Deprivation. Journal of Social Policy. 1987;16:25-46.
2. Benach J, Yasui Y. Geographical patterns of excess mortality in Spain explained by two indices of deprivation. Journal of Epidemiology and Community Health. 1999;53(7):423-31.
3. Carstairs V, Morris R. Deprivation: explaining differences in mortality between Scotland and England and Wales. BMJ. 1989;299(6704):886-9.
4. Lynch C, Holman CD, Moorin RE. Use of Western Australian linked hospital morbidity and mortality data to explore theories of compression, expansion and dynamic equilibrium. Australian health review : a publication of the Australian Hospital Association. 2007;31(4):571-81.
5. Newton JN, Briggs AD, Murray CJL, Dicker D, Foreman KJ, Wang H, et al. Changes in health in England, with analysis by English regions and areas of deprivation, 1990â€“2013: a systematic analysis for the Global Burden of Disease Study 2013. Lancet. 2015;386(10010):2257-74.
6. Carstairs V, Morris R. Deprivation and Health in Scotland. Aberdeen: Aberdeen University Press.; 1991.
7. Silke B. Deprivation as an Earlier Entry onto the Mortality Trajectory: Modelling Life Years Lost from Gompertz–Makeham Age Shift. British Journal of Healthcare & Medical Research (BJHMR). 2026;13(4):96-104.
8. Shalev I, Moffitt TE, Braithwaite AW, Danese A, Fleming NI, Goldman-Mellor S, et al. Internalizing disorders and leukocyte telomere erosion: a prospective study of depression, generalized anxiety disorder and post-traumatic stress disorder. Mol Psychiatry. 2014;19(11):1163-70.
9. Rey G, Jougla E, Fouillet A, Hémon D. Ecological association between a deprivation index and mortality in France over the period 1997 - 2001: variations with spatial scale, degree of urbanicity, age, gender and cause of death. BMC Public Health. 2009;9:33.
10. Brown D, Allik M, Dundas R, Leyland A. Carstairs Scores for Scottish Postcode Sectors, Datazones and Output Areas from the 2011 Census2014.
11. Pepper GV, Nettle D. Strengths, altered investment, risk management, and other elaborations on the behavioural constellation of deprivation. Behav Brain Sci. 2017;40:e346.
12. Kelly A, Teljeur C. SAHRU Deprivation Index Trinity College, Dublin2007 [Available from: https://www.drugsandalcohol.ie/34675/1/Trinity-deprivation-report-11-2019.pdf.
13. Sloggett A, Joshi H. Higher mortality in deprived areas: community or personal disadvantage? BMJ. 1994;309(6967):1470-4.